Preprint of the manuscript accepted to
15th International Workshop on Variable Structure
Systems and Sliding Mode Control (VSS18)

Use of second-order sliding mode observer for low-accuracy sensing in hydraulic machines

Michael Ruderman[1] and Leonid Fridman[2]

***Abstract*— Low-accuracy sensing is very common for the large hydraulic machines and does not allow for directly measuring the relative velocity which can be, otherwise, required for the control and monitoring purposes. This paper provides a case study of designing the second-order sliding mode observer based on the super-twisting robust exact differentiator. The nominal part of the system dynamics is derived from the simple available system measurements and incorporated into the observer structure. Parasitic by-effects, arising from the sensor sampling, quantization, and non-modeled distortions due to mechanical sensor interface, are shown as the main causes of hampering the final (steady-state) convergence of the observer states. Two cases – a continuous chirp excitation and a sequence of the short square pulses – are demonstrated for the open-loop motion experiments performed on a hydraulic crane, for which an accurate estimation of the motion system states is obtained.**

I. Foreword instead of introduction

Sliding mode control and observation techniques [1], [2], as particularly robust for the systems with uncertainties and disturbances, have gained attention in the various hydraulic applications, see e.g. more recent examples [3], [4], [5], [6] and several related articles in the issue [7]. A reliable real-time velocity estimation for the hydraulic machines with low-accuracy load position sensing belongs to essential problems of the control and monitoring during the operation. This note addresses that issue in the following case study.

II. Preliminaries

A. Robust exact differentiator

The robust exact differentiator [8], based on the super-twisting algorithm (STA) [9], aims for a real-time reconstruction of the state $x_2 = \dot{x}_1$, provided x_1 is the only available (measurable) system output. Furthermore, it is assumed that $|\ddot{x}_2| \leq L$ is the bounded perturbation, for some L to be a known constant. The state dynamics of the STA-based robust exact differentiator is given by

$$\begin{aligned} \dot{\hat{x}}_1 &= L^{1/2}\lambda_1 \, |x_1 - \hat{x}_1|^{1/2}\mathrm{sign}(x_1 - \hat{x}_1) + \hat{x}_2, \\ \dot{\hat{x}}_2 &= L\lambda_2 \, \mathrm{sign}(x_1 - \hat{x}_1), \end{aligned} \tag{1}$$

while $\hat{x}$ represents the estimate variable of the system state x. For the appropriately chosen parameters $\lambda_1, \lambda_2, L > 0$ the STA ensures the states convergence, i.e. $(x_1 - \hat{x}_1) = (x_2 - \hat{x}_2) = 0$, after a finite-time transient.

This work has received funding from the EUs H2020-MSCA-RISE research and innovation programme under grant agreement No 734832.

[1]M Ruderman is with Faculty of Engineering and Science, University of Agder (UiA), Norway, michael.ruderman@uia.no

[2]L Fridman is with Engineering Faculty, National Autonomous University of Mexico (UNAM), Mexico, lfridman@unam.mx

B. Second-order sliding mode observer

The second-order sliding mode observer, introduced in [10], extends the structure of an exact differentiator by explicitly taking into account the nominal part of the system dynamics $f(t, x_1, x_2, u)$. The overall system is assumed as

$$\begin{aligned} \dot{x}_1 &= x_2, \\ \dot{x}_2 &= f(t, x_1, x_2, u) + \xi(t, x_1, x_2, u), \\ y &= x_1, \end{aligned} \tag{2}$$

where x_1 is, again, the single available output (position) state. The exogenous control value is u – yet here out of interest since our focus is on the state observation, independently of the control loop. The system uncertainties, correspondingly perturbations, are concentrated in the term $\xi(\cdot)$. The suggested second-order sliding mode observer [10] has the form

$$\begin{aligned} \dot{\hat{x}}_1 &= \hat{x}_2 + z_1, \\ \dot{\hat{x}}_2 &= f(t, x_1, \hat{x}_2, u) + z_2. \end{aligned} \tag{3}$$

Note that the estimated state $\hat{x}_2$ appears as an argument variable when computing the nominal system dynamics. The correction variables of the super-twisting algorithm are

$$\begin{aligned} z_1 &= k_1|x_1 - \hat{x}_1|^{1/2}\mathrm{sign}(x_1 - \hat{x}_1), \\ z_2 &= k_2 \, \mathrm{sign}(x_1 - \hat{x}_1). \end{aligned} \tag{4}$$

According to [10], for an appropriate (k_1, k_2)-selection, the variables of observer (3) converge in finite time to the state variables of the system (2), i.e. $(\hat{x}_1, \hat{x}_2) \to (x_1, x_2)$.

III. Dynamic states of hydro-mechanic system

A. Approximated system dynamics

The transfer characteristics of the single cylinder-driven joint of a hydraulic machine can be approximated by

$$y(s) = G(s)s^{-1}\Phi[u(s)], \tag{5}$$

where the control value $u \in [-1, \ldots, 1]$ is subject to a static input nonlinearity Φ, and the cylinder stroke y is the measurable output quantity. The linear transfer function G, between the input and relative displacement rate, can be estimated from the measured frequency response; s is the Laplace variable. The input nonlinearity is associated, to the large part, with dead-zone of a directional control valve, used for operating the hydraulic cylinder, and is described by

$$\Phi[u] = \begin{cases} u - 0.5W\mathrm{sign}(u), & \text{if } |u| > 0.5W, \\ 0, & \text{else.} \end{cases} \tag{6}$$

Here the total input dead-band is denoted by W. Note that the approximated system dynamics (5), (6) largely neglect the residual nonlinear behavior of the control valve, hydraulic circuits, and mechanical subsystem. At the same time, a uniform harmonic excitation, over admissible frequency range, reveals an accurate match between the measured frequency response function (FRF) and (5). The measured FRF (details on the experimental system are given further in Section IV) and estimated transfer function characteristics $G(s)s^{-1}$ with

$$G(s) = \frac{15.59}{s^2 + 37.15s + 336} \tag{7}$$

are shown opposite to each other in Fig. 1. Here it is worth

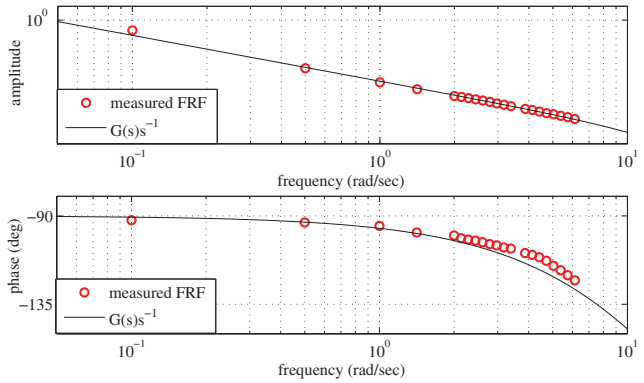

Fig. 1. Frequency response characteristics

noting that for a fast dynamics of directional control valves, a minimum phase second-order system G yields the best reasonable linear approximation. This is with regards to the continuity equations of hydraulic circuits, that introduce an additional integrator between the valve-controlled hydraulic flow and pressured-induced hydraulic force of the moving cylinder. Further we note that the input dead-band can be estimated either by an off- or on-line identification approach, see e.g. [11], [12], and that by various quasi-static open-loop control experiments. The overall identified dead-band of hydraulic system, used in this work, is $W = 0.6$. A

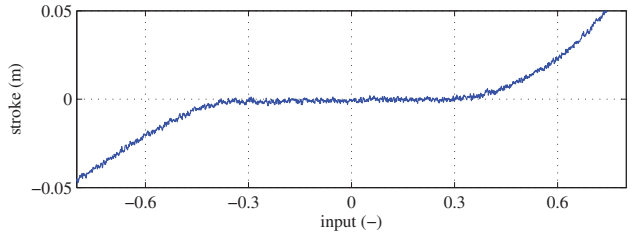

Fig. 2. Exemplary measured quasi-static input-output map with dead-zone

typical input-output map of the hydraulic cylinder, measured at the quasi-static excitation conditions with a flat input ramp, is exemplary shown in Fig. 2. Note that apart from a strongly-pronounced input dead-zone, another coupled by-effects of the non-modeled system behavior, like time lags, spool and piston stiction of the control valve and cylinder correspondingly, equally contribute to appearance of the dead-band in the input-output characteristics. However, a detailed and accurate decomposition of such locking and delaying sources in the motion dynamics are out of scope in the recent work and will be not further considered, this without lose of generality.

B. Observer design

The nominal part of the system dynamics to be used within the second-order sliding mode observer, cf. with (3), is given by the following differential equation

$$\dot{f} + 37.15f = 15.59\Phi[u] - 336\hat{x}_2. \tag{8}$$

That one is directly derived from the system approximation (5). Note that the nominal dynamics $f(\cdot)$ is not longer a function of available system output x_1. This is because x_1-state is not entering the overall motion dynamics which has one free integrator. Obviously, the latter is due to an unconstrained cylinder displacement, for which neither restoring forces (like dependent on the cylinder stroke) are in place.

The resulted sliding-mode observer, following the preliminaries given in sections II-A and II-B, has the form

$$\begin{aligned} \dot{\hat{x}}_1 &= L^{1/2}\lambda_1 \left|y - \hat{x}_1\right|^{1/2}\mathrm{sign}(y - \hat{x}_1) + \hat{x}_2, \\ \dot{\hat{x}}_2 &= L\lambda_2 \,\mathrm{sign}(y - \hat{x}_1) + f(t, \hat{x}_2, u). \end{aligned} \tag{9}$$

Since $\lambda_1 = 1.5$ and $\lambda_2 = 1.1$ can be directly assigned in advance, as an optimal setting for an exact differentiator according to [8], [13], the single remaining parameter of observer design is L. From the former exact differentiator developments, it is known that the gain selection should satisfy the single condition $|\ddot{y}| \leq L$, that is $L \geq C + K_M \sup|u|$. Here the input-output termed conditions are

$$\frac{\partial}{\partial u}\ddot{y} \leq K_M, \quad |\ddot{y}|_{u=0} \leq C,$$

cf. with [13]. It is evident that an appropriate observer gain selection requires the second time derivative of the output to be known. That one constitutes the acceleration of relative motion and is inherently unavailable once our goal is an observer-based estimation of the relative velocity. Comprehensibly, the prediction error of the nominal dynamics $f(\cdot, x_2) - f(\cdot, \hat{x}_2)$ and uncertainties $\xi(\cdot)$, both of the dimension of acceleration or generalized force, restrict the observer gain selection and, as consequence, the state convergence of observer (9).

Another optimal gain setting

$$k_2 = 1.1L, \quad k_1 = 2.028\sqrt{k_2},$$

recently proposed in [14], aims at minimizing the amplitude of fast-oscillations, i.e. chattering, caused by the presence of parasitic dynamics in the closed-loop of the super-twisting algorithm. To note is that the correspondingly determined k_1, k_2 gains are entering the observer equations as in (4) and not as in (9). Here again, L remains the single design parameter, yet unavailable for our system in the case study.

In the recent case study, the observer gains for both above mentioned optimal settings, i.e. according to [13] and [14],

are determined by using the measured system response and (numerically) solving the minimization problem

$$\min_{L} \sum_{i=1}^{N} \big(y_i - \hat{x}_{1,i}(L)\big)^2. \tag{10}$$

Here N is the full measured data set and $\hat{x}_{1,i}$ is the estimated position state as a function of variable L. The cumulative squared error is shown in Fig. 3 against the assigned L value. One can recognized that the optimal gain setting according

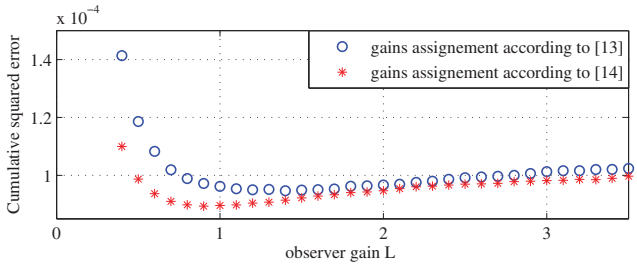

Fig. 3. Cumulative squared error against the observer gain, once with the gains assignments according to [13] and once according to [14].

to [14] performs slightly better in terms of the cumulative squared error. Following to that, the determined optimal $L = 0.9$ value is used for the gains setting, as provided in [14].

IV. Hydraulic loader crane

The experimental system used in the recent case study is a standard hydraulic loader crane with three rotary and one telescopic joints. For the sake of simplicity, and due to the operational space constraints, the third rotary joint only (the so-called jib joint) is under consideration for evaluating the sliding-mode observer. The jib joint connects the main boom and jib of the crane and is actuated by a linear stroke hydraulic cylinder mounted below the boom structure, cf. Fig. 4. For more details on the crane system see e.g. [11].

Fig. 4. Experimental setup of the hydraulic loader crane

The external communication interface to the integrated circuits cabinet is based on the Ethernet connection with UDP (user datagram protocol). The real-time sampling rate is set to be sufficiently high, 1 kHz. Yet, the accessible encoder values, which reflect the linear stroke of hydraulic cylinders, are digitally processed (onside of the circuits cabinet) at a lower sampling rate. In addition, this yields as not fully deterministic so that the sampling period of the updated encoder values vary between 6 msec and 12 msec, cf. Fig. 5.

The cylinder stoke values are also subject to the quantization, while an exact (nominal) value of the quantization step remains unavailable. Furthermore, it should be emphasized that the measured cylinder strokes are provided by encoders connected to the moving links via the prestressed steel wires of a relatively high length. This hardware solution, which is quite common for the large-scale hydraulic cranes working in the outside environments, gives rise to additional perturbations of the measured cylinder stroke. All the above mentioned (parasitic) by-effects can be seen as the output measurement noise which aggravates observation of the velocity state we are interested in. The measured cylinder stroke, with the clearly visible sampling and quantization perturbations, is exemplarily shown in Fig. 5. Note that here a steady-state motion at the low excitation conditions has been realized. Also it should be noted, for a better system overview, that the full cylinder stroke is about 0.85 m.

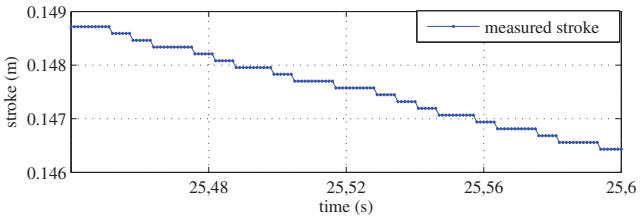

Fig. 5. Exemplarily measured cylinder stroke at steady-state motion

V. Observer evaluation

The second-order sliding mode observer, designed according to the section III-B, has been experimentally evaluated on the motion responses of the jib joint which is driven by the hydraulic cylinder, cf. section IV.

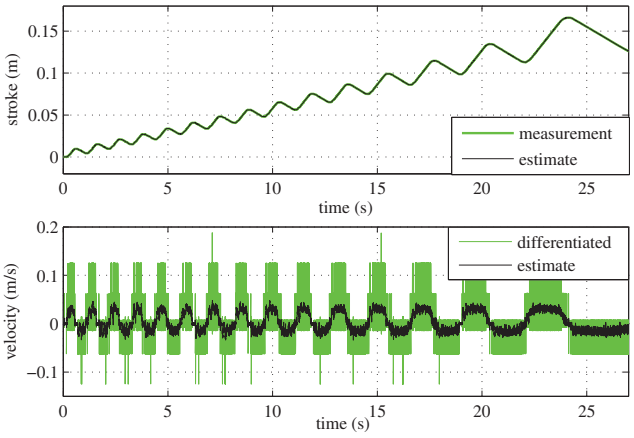

Fig. 6. Estimated and real motion response to the chirp control sequence: cylinder stroke above, and relative velocity below

First, the open-loop control signal is given by a down-chirp sequence, starting from 1 Hz and decreasing towards 0.25 Hz during 27 seconds. The estimated and measured motion response are shown opposite to each other in Fig. 6. The upper plot discloses the cylinder stroke while the lower plot shows the relative velocity. One can see that the

cylinder stoke is subject to a continuous drift which can be attributed to the asymmetric (one-rod) hydraulic cylinder and additional impact of gravity; both are not captured by the approximated motion dynamics (5)-(7). Further we note that no real reference measurements of the relative velocity are available and, therefore, an equivalent value only is obtained from the encoder signals by a discrete-time differentiation. With respect to the control bandwidth of directional control valve and for the sake of an easier signals interpretation, the depicted x_2, which is equivalent to the measured velocity, is low-pass filtered with the cut-off frequency at 200 Hz.

As next, a sequence of the square pulses of 0.5 sec length is applied as an open-loop control signal. The measured and observer-estimated motion response is shown in Fig. 7, the cylinder stroke above and the relative velocity below. Here again, the differentiated value of relative velocity is low-pass filtered as mentioned above. One can see that at

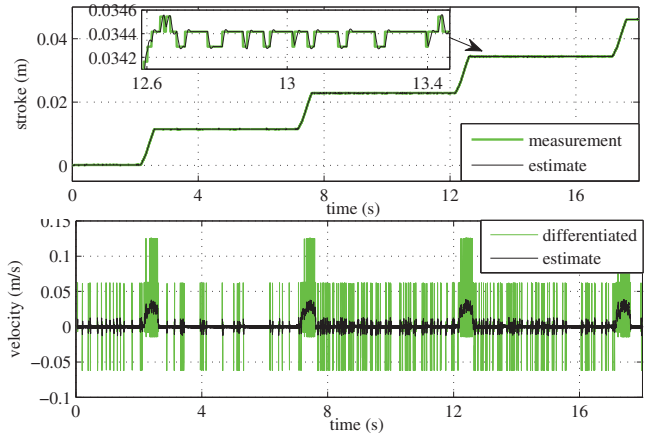

Fig. 7. Estimated and real motion response to the square pulses control sequence: cylinder stroke above, and relative velocity below

each square pulse the system exhibits a transient response, following by an idle phase until the next pulse applies. An aperiodic pattern of a flipping-bit character appears during each idle phase, cf. zoom-in in Fig. 7 above. One can see that the designed observer is able to follow the measured position state within the flipping-bit. Also the observer-corrected, i.e. with $\hat{x}_2$-argument, nominal system dynamics f is shown in Fig. 8 as a function of time. One can recognize that

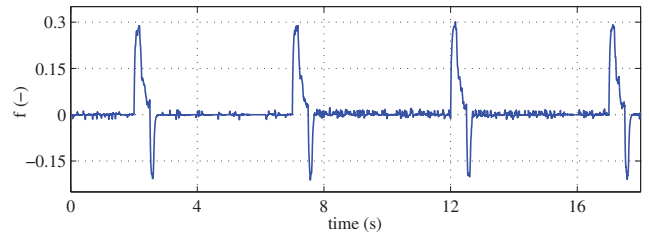

Fig. 8. Observer-corrected nominal system dynamics $f(t, \hat{x}_2, u)$

the f-trajectory, which is proportional to hydraulic force and, therefore, pressure difference across the cylinder piston, is relatively smooth and without hight-frequent oscillating pattern. That is essential for e.g. feedback linearization.

VI. Summary

In this paper, we have presented a case study of applying the second-order sliding mode observer for estimating the relative velocity in hydraulic machines with low-accuracy sensing. The robust exact differentiator based on the super-twisting algorithm has been augmented by the nominal part of the system dynamics. The latter has been derived and identified for our hydro-mechanical system by using a simple set of the limited experimental data, without special measurements and system decompositions. Two optimal gain settings have been used for parameterizing the state observer, while the L-gain has been obtained by numerically solving the squared error minimization problem. The designed second-order sliding mode observer has been experimentally evaluated for the rotary jib joint of a standard loader crane, actuated by the linear hydraulic cylinders. An accurate state estimation has been shown for different measured motion responses. Furthermore, the observer-corrected nominal system dynamics, which is equivalent to the driving hydraulic force, showed up the sufficiently smooth trajectory. That appears promising for the future works towards the sliding mode observer-based full-order state feedback control – relevant for hydraulic machines with a low-accuracy output sensing.

References

[1] Y. Shtessel, C. Edwards, L. Fridman, and A. Levant, *Sliding mode control and observation*. Springer, 2014.

[2] V. Utkin, J. Guldner, and J. Shi, *Sliding mode control in electro-mechanical systems*. CRC press, 2009.

[3] J. Komsta, N. van Oijen, and P. Antoszkiewicz, "Integral sliding mode compensator for load pressure control of die-cushion cylinder drive," *Control Engineering Practice*, vol. 21, no. 5, pp. 708–718, 2013.

[4] C. Vázquez, S. Aranovskiy, L. B. Freidovich, and L. M. Fridman, "Time-varying gain differentiator: A mobile hydraulic system case study," *IEEE Transactions on Control Systems Technology*, vol. 24, no. 5, pp. 1740–1750, 2016.

[5] S. Koch and M. Reichhartinger, "Observer-based sliding mode control of hydraulic cylinders in the presence of unknown load forces," *Elektrotechnik und Informationstechnik*, vol. 133, pp. 253–260, 2016.

[6] L. Schmidt, T. O. Andersen, P. Johansen, and H. C. Pedersen, "A robust control concept for hydraulic drives based on second order sliding mode disturbance compensation," in *ASME/BATH 2017 Symposium on Fluid Power and Motion Control*, 2017.

[7] M. Horn and M. Steinberger, "Sliding mode applications on hydraulics and pneumatics," *e & i Elektrotechnik und Informationstechnik*, vol. 133, no. 6, pp. 237–237, 2016.

[8] A. Levant, "Robust exact differentiation via sliding mode technique," *Automatica*, vol. 34, no. 3, pp. 379–384, 1998.

[9] A. Levant, "Sliding order and sliding accuracy in sliding mode control," *Int. journal of control*, vol. 58, no. 6, pp. 1247–1263, 1993.

[10] J. Davila, L. Fridman, and A. Levant, "Second-order sliding-mode observer for mechanical systems," *IEEE transactions on automatic control*, vol. 50, no. 11, pp. 1785–1789, 2005.

[11] M. H. Rudolfsen, T. N. Aune, O. Auklend, L. T. Aarland, and M. Ruderman, "Identification and control design for path tracking of hydraulic loader crane," in *IEEE International Conference on Advanced Intelligent Mechatronics (AIM)*, 2017, pp. 565–570.

[12] M. Ruderman, "Minimal-model for robust control design of large-scale hydraulic machines," in *IEEE International Workshop on Advanced Motion Control (AMC)*, 2018, pp. 397–401.

[13] A. Levant, "Principles of 2-sliding mode design," *Automatica*, vol. 43, no. 4, pp. 576–586, 2007.

[14] U. P. Ventura and L. Fridman, "Is it reasonable to substitute discontinuous smc by continuous hosmc," *arXiv*, 2017. [Online]. Available: https://arxiv.org/pdf/1705.09711.pdf